Thomson Scattering from Ultrashort and Ultraintense Laser Pulses

Ju Gao*

ECE Department, University of Illinois, Urbana, Illinois 61801, USA

(Received 12 April 2004; published 6 December 2004)

The Thomson scattering in an ultraintense ($\sim 10^{18}$ W cm^{-2}) and ultrashort (20 fs) laser field is calculated that demonstrates different characteristics from those of the low-intensity field case. The electron trajectory no longer conforms to a figure-eight pattern, and the spectra demonstrate complex shifting and broadening to suggest that Thomson scattering can be used for characterizing pulsed lasers. The initial phase at the electron entrance of the field can critically affect the Thomson scattering, but its effect is weighted by the intensity profile of the field. As a result, the fourfold symmetry of the radiation pattern breaks down when the electron enters the field closer to the pulse peak. The relationship between the Thomson scattering and Compton scattering in the high field is analyzed.

DOI: 10.1103/PhysRevLett.93.243001 PACS numbers: 32.80.Cy, 03.50.De, 41.60.Cr, 42.50.Hz

Introduction.—Rapid progress in producing ultraintense laser fields has created an emerging high-field physics, and the electron-photon interaction is at the core of the subject. For example, Thomson scattering in intense laser fields has shown much more complex characteristics [1–4] than scattering in weaker fields.

Thomson scattering and Compton scattering are used to describe the process of light scattering from a free electron. In the low-field regime, Thomson scattering can be considered as the low-energy limit of Compton scattering, focusing only on the wave aspect of the field. In the high-field regime, the photon aspect may not be completely neglected even if the photon energy is low, because the electron can coherently interact with a large number of photons. Therefore, before we focus our discussion on the Thomson scattering, we will evaluate the distinction between the two processes in an ultraintense field.

The distinction between strong field-electron scattering and its weak field counterpart lies in the number of photons with which the electron can simultaneously interact. Note that the electron cannot interact with all photons in the field but only with a number of coherent-interacting or "dressed" photons in a volume defined by characteristic lengths of both the field and electron, the wavelength λ and the electron classical radius r_e. With the photon density given by $\rho = \frac{n}{V_\gamma}$, the number of the dressed photons z is then $z = C r_e \lambda^2 \frac{n}{V_\gamma}$, where C is a geometric factor. Assuming $C = \frac{1}{2\pi}$, the total energy of the dressed photons becomes

$$U_p \equiv z\hbar\omega = \frac{1}{2\pi} r_e \lambda^2 \frac{n}{V_\gamma} \hbar\omega, \tag{1}$$

which is exactly the ponderomotive energy derived from the quantum electrodynamic theory [5]. The expression reduces to the classical definition of ponderomotive energy by letting $\frac{n}{V_\gamma}\hbar\omega c = I$, where c is the speed of light and I is the laser intensity. At high intensity (10^{14} W cm^{-2} and above), the ponderomotive energy U_p becomes indispensable in the energy conservation for any laser-matter interaction processes, e.g., above threshold ionization (ATI) and high-order harmonic generation, because its value already exceeds the single photon energy $\hbar\omega$.

A momentum counterpart of the ponderomotive energy should exist that can be defined as the total momentum of the dressed photons, $\mathbf{P}_p \equiv z\hbar\mathbf{k}$ that is parallel to the individual photon momentum. The ponderomotive four-momentum is thus formed:

$$(U_p, \mathbf{P}_p) \equiv zk = z(\hbar\omega, \hbar\mathbf{k}), \tag{2}$$

which is on the light cone ($|\mathbf{P}_p| = cU_p$) rather than the electron mass shell [6].

The emergence of the ponderomotive four-momentum ensures a qualitative difference for the electron-photon scattering process because it enters the four-momentum conservation equation. In other words, the dressed electron has to be treated differently from a free electron. We first consider the process of injecting a free electron into the inside of the field whose four-momentum conservation is expressed by

$$P_i + lk = P + nk + zk + k_1', \tag{3}$$

where $P_i = (\gamma_0 mc^2, \gamma_0 m\mathbf{v})$ and $P = (\gamma mc^2, \gamma m\mathbf{v})$ are the electron four-momentum before and after it enters the field, and $\gamma = 1/\sqrt{1 - (\mathbf{v}/c)^2}$. Here l, n are the photon numbers of the field before and after the electron enters the field, respectively, and k_1' is the four-momentum of the secondary photon. Equation (3) can be simplified to

$$P_i + (j - z)k = P + k_1', \tag{4}$$

where $j \equiv l - n$ is the number of photons absorbed to account for the change of electron four-momentum $P - P_i$, generation of a spontaneous photon k_1', and the acquiring of the ponderomotive four-momentum zk. In the high-field regime, z is large, e.g., $z \sim 10^{4-5}$ for intensity $\sim 10^{18}$ W cm^{-2}; therefore j is also large. This high-order multiphoton process cannot be reduced to the case of Thomson scattering.

Experimentally, it is found that injecting free electrons into the high-field region is difficult as the ponderomotive energy can repel the electrons. The process is understood as ponderomotive scattering [7]. One way to overcome ponderomotive scattering is to produce the electrons through ionization so that the free electron is born within the field [3,8]. We will assume this ionization condition and leave the discussion of ponderomotive scattering to another treatise. However, we would like to point out that a resonant ponderomotive scattering exists for $z =$ integer, i.e., when the ponderomotive energy is an integer multiple of the photon energy. Referring to Eq. (4), at this resonant condition the electron can tunnel into the field ($P = P_i$) without creating a spontaneous photon (k_1'), similar to the resonant effect predicted for the electron exiting the field during an ATI process [9].

Now that the electron is completely within the laser field and has gained the ponderomotive four-momentum, the new four-momentum conservation is given by

$$P + nk + zk = P' + mk + zk + k_2', \tag{5}$$

where k_2' is another spontaneous photon emitted inside the laser field and P' is the four-momentum of the electron due to the recoil. Notice Eq. (5) becomes

$$P + j'k = P' + k_2', \tag{6}$$

where the photon absorption $j' \equiv n - m$ can be a small number after canceling the large ponderomotive terms. At low photon energy, the process described by Eq. (6) can thus be regarded as the low-energy limit of the Compton scattering, even for ultraintense field values.

Our conclusion is that the high-field-electron interaction process must be divided into a Compton-like ponderomotive scattering, in which the electron penetrates and leaves the field, and a Thomson scattering once the electron is within the field. Only the radiation from the electron within the field is treatable by the classical electrodynamics, while the ponderomotive scattering process may have to be calculated via a quantum electrodynamic formalism. The nonlinear Thomson scattering experiment [3] shows that the dominant radiation is from the electron in the field.

Electron trajectory.—The classical approach to the Thomson scattering is a straightforward two-step calculation: First, use Newton's laws to find the electron trajectory, and then use Maxwell's equations to calculate the radiation. Only recently has the theory been extended to an ultraintense field to address such topics as the figure-eight motion, harmonic generation, and the initial phase effects [1,2,10–12], and the work on a high-field pulsed laser has just begun [13].

The electron trajectory in the field is governed by the relativistic equations of motion:

$$\frac{d\mathbf{P}}{dt} = q[\mathbf{E}(\mathbf{r}, t) + \mathbf{v} \times \mathbf{B}(\mathbf{r}, t)], \quad \frac{dE}{dt} = q\mathbf{v} \cdot \mathbf{E}(\mathbf{r}, t), \tag{7}$$

where $\mathbf{P} = \gamma m\mathbf{v}$ and $E = \gamma mc^2$. A linearly polarized (in the x direction) laser pulse traveling in the z direction is described by $\mathbf{E}(\mathbf{r}, t) = f(t - \hat{\mathbf{k}} \cdot \mathbf{r}/c)\hat{x}\cos(\omega t - \mathbf{k} \cdot \mathbf{r} + \Theta)$, where $f(t - \hat{\mathbf{k}} \cdot \mathbf{r}/c)$ is the pulse shape function. A Gaussian pulse is assumed as $f(t - \hat{\mathbf{k}} \cdot \mathbf{r}/c) = \exp[-4\ln(2) \times (t - \hat{\mathbf{k}} \cdot \mathbf{r}/c)^2/T^2]$, where T is the pulse width. The magnetic field relates to the electric field by $\mathbf{B}(\mathbf{r}, t) = \frac{1}{c}\mathbf{E}(\mathbf{r}, t)$. Θ is the initial phase of the laser field, which is determined by the laser field and can be set to zero. Θ is different from the initial phase that the electron sees when it enters the field, which we denote as the entrance initial phase or entrance phase $\tau_0 \equiv \omega t_0 - \mathbf{k} \cdot \mathbf{r}(t_0)$. τ_0 has been shown to have significant effects on Thomson scattering in a continuous field [12,14]; however, in a pulse field, its role has to be weighted by the pulse function $f(t - \hat{\mathbf{k}} \cdot \mathbf{r}/c)$. The detailed analysis will be presented in the section *Phase dependence*.

Equations (7) can be solved numerically, given the pulse shape. It is to be noted that the term $\mathbf{k} \cdot \mathbf{r}$ inside $\cos(\omega t - \mathbf{k} \cdot \mathbf{r})$ is not fixed due to the ponderomotive momentum and has to be solved for simultaneously with Eqs. (7) to give the correct local field strength on the electron. In the following calculation, the laser field is chosen to have a center wavelength of $\lambda = 1\ \mu$m and a pulse width of 20 fs with a peak intensity of $10^{18}\ \mathrm{W\,cm^{-2}}$. We assume the electron is born still inside the field well before the peak arrives, i.e., $v_x(t_0) = 0; v_z(t_0) = 0$ at $t_0 = -4T$.

Figure 1 shows the velocity waveforms of the electron in both transverse (x-axis) and forward (z-axis) directions. At the given intensity, the electron is driven to relativistic speed in both directions, which is of interest for laser acceleration. However, the electron loses its gained momentum at the tail of the pulse; therefore, it is a challenge to preserve the high momentum the electron acquires from the laser field once it leaves the field.

The longitudinal motion oscillates with twice the frequency of the transverse motion, which results in second harmonic generation. The electron never moves backwards, and the mean value of the oscillation corresponds to the ponderomotive momentum [6] that causes the oscillation frequency to be lower than the laser frequency. This would predict a redshift of the radiation spectra.

Figure 2 shows the electron trajectory. We plot $x(t)$ versus $z(t)$, with $x(t_0) = 0$ and $z(t_0) = 0$. Notice that the presumed figure-eight trajectory cannot be realized because the electron never moves backward. The breakdown of the figure-eight pattern is also manifested by the sharp edges in the trajectory in Fig. 2, which was also demonstrated both theoretically [13] and experimentally [15] in previous works.

Radiation spectra.—Now that the electron motion is known, the radiation phenomena are described by the Lienard-Wiechert theorem. The energy radiated per unit solid angle per unit frequency interval [16] is given by

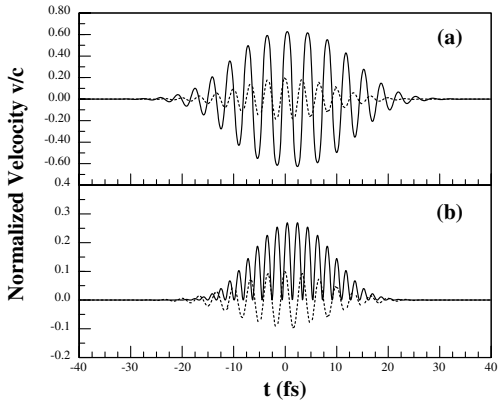

FIG. 1. Velocity waveforms normalized by the speed of light in (a) transverse and (b) forward directions for a 1 μm wavelength and 20 fs pulsed field with peak intensity 10^{18} W cm^{-2}. The waveform of the laser field observed at a fixed position is also shown (dotted line) in arbitrary units for comparison of the phases.

$$\frac{d^2W}{d\omega d\Omega} = \frac{e^2\omega^2}{4\pi^2c^3}\left(\int_{-\infty}^{\infty} dt\{\mathbf{n}\times[\mathbf{n}\times\mathbf{v}(t)]\} \times \exp\{i\omega[t-\mathbf{n}\cdot\mathbf{r}(t)/c]\}\right)^2, \quad (8)$$

where $\mathbf{n}$ is the unit vector directed from the origin to the observation point. Both $\mathbf{v}(t)$ and $\mathbf{r}(t)$ are measured in the laboratory frame, so the solution of Eqs. (7) can be used directly.

Figure 3 shows the radiation spectra of back scattering ($\theta = 180°$; see the inset for the polar coordinate) from the same laser pulse in Fig. 1 and $t_0 = -4T = -80$ fs. As in the continuous field case with zero entrance phase, only the odd harmonics are produced [12], but with significant redshift. The higher order harmonics have greater frequency shifts, and all harmonics shift more at higher intensity. The spectra are broader than the transform-limited width of the laser field, with the maximum shifts corresponding to the peak intensity. The extremely broadened harmonic spectra resemble those observed experimentally [3]. The multiple-peak structure is likely due to the coherent relation between the transverse and longitudinal motions. These spectral details suggest that Thomson scattering can be used to characterize the ultrashort and ultraintense laser field.

A question arises as to how to discern harmonics when the broadening causes them to overlap. The problem can be partially solved if we move the observation point away from the backward direction. In general, observers positioned at small values of the angle θ observe less spectral broadening at a given intensity. Equation (9) relates the broadening to the peak intensity I_{peak} and wavelength at different observation angles θ,

$$\Delta\omega = -n\omega_0\left[\frac{(1-\cos\theta)(1/2\pi c)r_e\lambda^2 I_{\text{peak}}}{\gamma_0 mc^2 + (1-\cos\theta)(1/2\pi c)r_e\lambda^2 I_{\text{peak}}}\right], \quad (9)$$

where n is the harmonic order. Notice that a high intensity pulse spreads the harmonics down to much lower frequencies so that the Thomson scattering might be exploited as a novel "lower frequency," such as THz, radiation source.

Phase dependence.—The entrance initial phase, defined as the phase the electron sees when it enters the field, can critically affect the electron trajectory in a continuous field [12,14]. For a pulse, however, one would argue that if the electron intercepts the field well before the peak arrives, any phase effects have to be minimized due to causality. This suggests that the dependence on the phase should be weighted by the pulse profile. A mathematical analysis of the above statement is outlined here. The symbolic solution to Eqs. (7) can be expressed by

$$\mathbf{P}(t) = \mathbf{P}(t_0) + \int_{t_0}^{t} dt' q f(t')[\hat{\mathbf{x}}\cos(\omega t' - \mathbf{k}\cdot\mathbf{r}) + (\mathbf{v}\times\hat{\mathbf{x}})\cos(\omega t' - \mathbf{k}\cdot\mathbf{r})]/c. \quad (10)$$

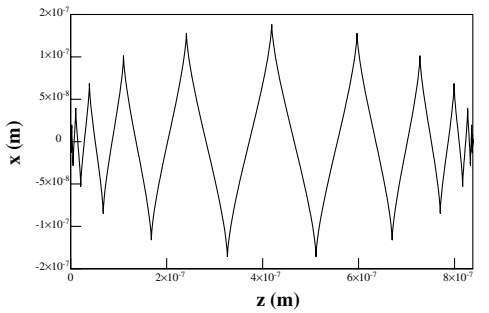

FIG. 2. The electron trajectory observed from the laboratory frame does not follow figure-eight pattern. The laser field is the same as that in Fig. 1.

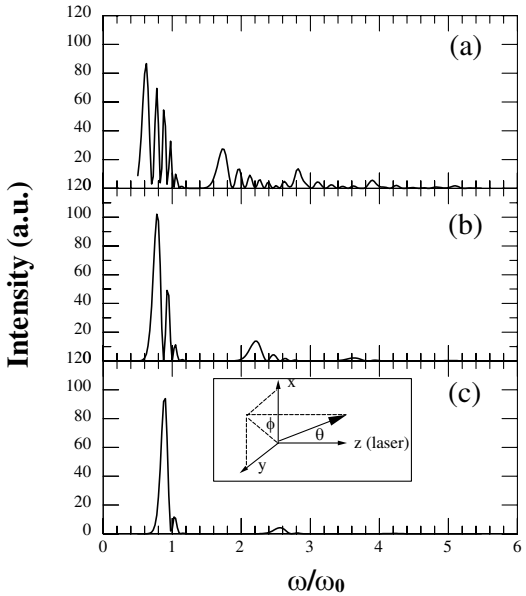

FIG. 3. Spectrum for 1 μm, 20 fs laser pulse with peak intensity (a) 2×10^{18} W cm^{-2}, (b) 1×10^{18} W cm^{-2}, and (c) 5×10^{17} W cm^{-2}.

Knowing that $f(t)$ oscillates more slowly than the field itself, the above equation can be reduced to the first order approximation:

$$\mathbf{P}(t) = \mathbf{P}(t_0) + q[f(t)G(t) - f(t_0)G(t_0)], \qquad (11)$$

where the function $G(t') = \int dt'[\hat{\mathbf{x}}\cos(\omega t' - \mathbf{k}\cdot\mathbf{r}) + (\mathbf{v}\times\hat{\mathbf{x}})\cos(\omega t' - \mathbf{k}\cdot\mathbf{r})]/c$ is also fast oscillating. Therefore the dynamics of the electron is dependent, sensitively, on the initial phase $\tau_0 \equiv \omega t_0 - \mathbf{k}\cdot\mathbf{r}(t_0)$ at the time the electron is born t_0. However, $G(t_0)$, which represents the initial phase effect, is weighted by the pulse function $f(t_0)$. Thus, the initial phase effect is maximum if the electron intercepts the field close to the pulse peak, and diminishes if the electron is created within the field well before the peak arrives.

Symmetry breakdown.—Here we predict an asymmetry in the presumed fourfold symmetrical azimuthal radiation pattern. The linear polarized field assures the reflection symmetry along the polarization $\phi = 0°$ axis. Symmetry about the $\phi = 90°$ axis is usually assumed because the electron spends virtually the same amount of time interacting with the up and down sense of the field. However, this assumption may not hold for an ultrashort and ultraintense laser field where the electron can interact much longer relatively with the field in one sense than the other. As a result, the fourfold symmetry is reduced to twofold symmetry about the polarization axis.

Figure 4 shows the azimuthal angular distribution for the electron entering the field at different times. When the electron enters the field well before the peak arrival ($t_0 = -4T$), the radiation demonstrates the fourfold symmetry. However, when the electron is born in the field much closer to the peak arrival ($t_0 \simeq -T$), only the symmetry along the $\phi = 0°$ axis is preserved.

In experiments [3], multiple electrons entering the field at different times spread the entrance phases, causing the radiation to appear as fourfold symmetry. Symmetry breakdown may be observed by using a single electron or a prebunched electron beam. It is possible that the broken symmetry can be utilized to pinpoint the "birth time" of the free electron inside the laser field.

Conclusion.—In this work, we investigated the electron interaction with an ultraintense and ultrashort laser pulse. We presented the analysis to justify the classical theory treatment of the Thomson scattering in the high field, provided that the radiation during the electron entering and leaving the field is excluded. The calculated dynamics and emission of the electron inside the field reveal the presence of the ponderomotive momentum. The fourfold symmetry of the spatial distribution can be broken, with the outcome depending on the initial phase and the position of the pulse envelope at the time the electron is created in the field. These results suggest that the Thomson scattering can be employed to characterize the ultraintense and ultrashort laser fields and to study the ultrafast dynamics of the electrons.

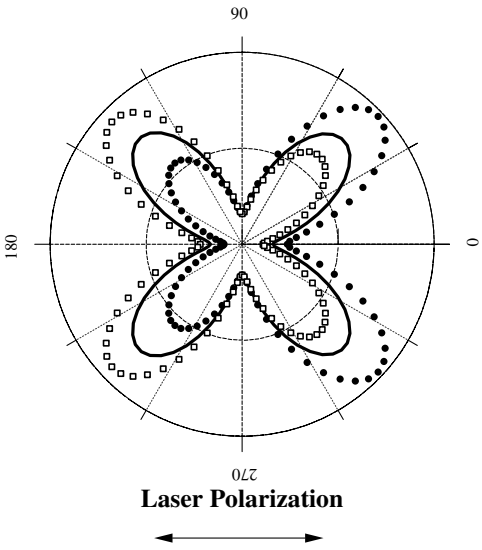

FIG. 4. Azimuthal angular distribution observed at $\theta = 90°$ and $\omega = 2\omega_0$ for the electron entrance time at $t_0 = -4T$ (solid line), $t_0 = -T$ (●), and $t_0 = -1.008T$ (□). As indicated, the polarization is along the $\phi = 0°$ direction. The laser pulse is 1 μm and 20 fs with peak intensity $1 \times 10^{18}\,\mathrm{W\,cm^{-2}}$.

The author would like to thank F. Shen for stimulating discussions and J. Palkovic and E. Ebert for carefully reviewing the manuscript.

*Electronic address: jugao@uiuc.edu

[1] R. W. Boyd, *Nonlinear Optics* (Acadmic, Boston, 1992).
[2] E. V. Hartemann, *High Field Electrodynamics* (CRC Press, Boca Raton, FL, 2001).
[3] S. Y. Chen, A. Maksimchuk, and D. Umstadter, Nature (London) **396**, 653 (1998).
[4] M. H. Walser, C. H. Keitel, A. Scrinzi, and T. Brabec, Phys. Rev. Lett. **85**, 5082 (2000).
[5] D. Guo and T. Aberg, J. Phys. A **21**, 4577 (1988).
[6] J. Gao, D. Bagayoko, and D. S. Guo, Can. J. Phys. **76**, 87 (1998).
[7] P. H. Bucksbaum, M. Bashkansky, and T. J. McIlrath, Phys. Rev. Lett. **58**, 349 (1987).
[8] S. Augst, D. Strickland, D. D. Meyerhofer, S. L. Chin, and J. H. Eberly, Phys. Rev. Lett. **63**, 2212 (1989).
[9] J. Gao, D. S. Guo, and Y. S. Wu, Phys. Rev. A **61**, 043406 (2000).
[10] E. S. Sarachik and G. T. Schappert, Phys. Rev. D **1**, 2738 (1970).
[11] E. Esarey, S. Ride, and P. Sprangle, Phys. Rev. E **48**, 3003 (1993).
[12] F. He, Y. Y. Lau, D. P. Umstadter, and T. Strickler, Phys. Plasmas **9**, 4325 (2002).
[13] G. A. Krafft, Phys. Rev. Lett. **92**, 204802 (2004).
[14] J. E. Gunn and J. P. Ostriker, Astrophys. J. **165**, 523 (1971).
[15] K. J. Kim, in *Characteristics of Synchrotron Radiation*, AIP Conf. Proc. No. 184 (AIP, New York, 1989), p. 565.
[16] J. D. Jackson, *Classical Electrodynamics* (Wiley, New York, 1962).